by the structure of silanol, namely, bulkiness around SiOH and SiOH acidity. Tris-2-naphthylsilyl *tert*-butyl peroxide had the best photodecomposition rate and initiation rate.

Registry No. ANaCH-Cl, 65787-77-1; ANa2Ph-H, 100447-84-5; ANa2Ph-Br, 100447-85-6; ANa2Ph-Bu, 100447-86-7; MePh2Ph-Bu, 100447-87-8; 3BNa-Bu, 100447-88-9; 3ClPh-Bu, 94780-15-1; 2ANa-Bu, 100447-89-0; 3Ph-Cu, 31731-51-8; 3ClPh-OH, 18373-61-0; 3ANa-OH, 18919-22-7; 2ANa-2OH, 18676-77-2; ANa2Ph-OH, 100447-90-3; MePh2Ph-OH, 736-71-0; 3Ph-Bu, 18751-58-1; 2Ph-2-Bu, 15188-08-6; 3Ph-OH, 791-31-1; $Al(etaa)_3$, 15306-17-9; 2Ph-2OH, 947-42-2; $HSiCl_3$, 10025-78-2; *t*-BuOOH, 75-91-2; $SiCl_4$, 10026-04-7; 1-naphthyl bromide, 90-11-9; diphenyldichlorosilane, 80-10-4; diphenylchlorohydrosilane, 1631-83-0; 1-naphthylmagnesium bromide, 703-55-9; *N*-bromosuccinimide, 128-08-5; tri-2-naphthylsilane, 100447-91-4; 2-naphthyl bromide, 580-13-2; tris(4-chlorophenyl)silane, 6485-82-1; (4-chlorophenyl)magnesium bromide, 873-77-8; di-1-naphthyldichlorosilane, 18676-65-8; triphenylsilyl chloride, 76-86-8; cumyl hydroperoxide, 80-15-9; tris(4-chlorophenyl)silyl bromide, 18557-72-7; tri-2-naphthylsilanol, 100447-92-5; cyclohexene oxide, 286-20-4; cyclohexene oxide (homopolymer), 25702-20-9.

References and Notes

(1) Pappas, S. P. *Photogr. Sci. Eng.* **1979**, *23*, 140.
(2) Watt, W. R. US Patent 3 721 616.
(3) Watt, W. R. US Patent 3 794 576, 1974.
(4) Watt, W. R. US Patent 3 816 280, 1974.
(5) Licari, J. J. US Patent 3 205 157.
(6) Schelessinger, S. I. US Patent 3 708 296, 1973.
(7) Crivello, J. V.; Lam, J. H. W.; Moore, J. E.; Schroster, S. H. *J. Radiat. Curing* **1978**, *5*, 2.
(8) Crivello, J. V.; Lam, J. H. W. *Macromolecules* **1977**, *10*, 1307.
(9) Crivello, J. V.; Lam, J. H. W. *J. Polym. Sci., Polym. Chem. Ed.* **1979**, *17*, 2877.
(10) Crivello, J. V.; Lam, J. H. W. *J. Polym. Sci., Polym. Chem. Ed.* **1979**, *17*, 1047.
(11) Crivello, J. V.; Lam, J. H. W. *J. Polym. Sci., Polym. Chem. Ed.* **1980**, *18*, 1021.
(12) Crivello, J. V.; Lam, J. H. W. *J. Polym. Sci., Polym. Chem. Ed.* **1979**, *17*, 977.
(13) Crivello, J. V.; Lam, J. H. W. *J. Polym. Sci., Polym. Chem. Ed.* **1978**, *16*, 2441.
(14) Ledwith, A. *Makromol. Chem., Suppl.* **1979**, *3*, 348.
(15) Ledwith, A.; Al-Kass, S.; Hulme-Lowe, A. *Cationic Polym. Relat. Processes, Proc. Int. Symp., 6th* **1983**, 275.
(16) Watt, W. R.; Hoffman, H. T., Jr; Pobiner, H.; Schkolnick, L. J.; Yang, L. S. *J. Polym. Sci., Polym. Chem. Ed.* **1984**, *22*, 1789.
(17) Pappas, S. P.; Gatechair, L. R.; Jilek, J. H. *J. Polym. Sci., Polym. Chem. Ed.* **1984**, *22*, 77.
(18) Pappas, S. P.; Gatechair, L. R.; Jilek, J. H. *J. Polym. Sci., Polym. Chem. Ed.* **1984**, *22*, 69.
(19) Hayase, S.; Onishi, Y.; Suzuki, S.; Wada, M. IUPAC, 6th International Symposium on *Cationic Polym. Relat. Processes, Int. Symp., 6th* **1983**, 115; *Macromolecules* **1985**, *18*, 1799.
(20) Berg, E. W.; Herrera, N. M. *Anal. Chim. Acta.* **1972**, *60*, 117.
(21) Buncel, E.; Daries, A. G. *Chem. Ind. (London)* **1956**, 1052.
(22) Fan, Y. L.; Shaw, R. G. *J. Org. Chem.* **1973**, *38*, 2410.
(23) Hatchard, C. G.; Parker, C. A. *Proc. R. Soc. London, A* **1956**, *235*, 518.
(24) Hatchard, G. G.; Parker, C. A. *Proc. R. Soc. London, A* **1953**, *220*, 104.
(25) Murov, S. L. "Handbook of Photochemistry"; Marcel Dekker: New York, 1973, p 119.
(26) Hayase, S.; Ito, T.; Suzuki, S.; Wada, M. *J. Polym. Sci., Polym. Chem. Ed.* **1981**, *19*, 2185.
(27) Hayase, S.; Ito, T.; Suzuki, S.; Wada, M. *J. Polym. Sci., Polym. Chem. Ed.* **1981**, *19*, 2977.
(28) Hayase, S.; Ito, T.; Suzuki, S.; Wada, M. *J. Polym. Sci., Polym. Chem. Ed.* **1982**, *20*, 3155.
(29) Dannley, R. L.; Jalics, G. *J. Org. Chem.* **1965**, *30*, 3848.
(30) Eaborn, C.; Jackson, R. A.; Pearch, R. *Chem. Commun.* **1967**, 920.

Compatibility of Substituted Phenol Condensation Resins with Poly(methyl methacrylate)

John R. Pennacchia, Eli M. Pearce,* T. K. Kwei, Bernard J. Bulkin, and Jong-Pyng Chen

Polymer Research Institute, Polytechnic Institute of New York, Brooklyn, New York 11201, and Materials Research Laboratory, Industrial Technology Research Institute, Hsinchu, Taiwan.

Received June 25, 1985

ABSTRACT: Polymer blends based on proton donor-acceptor interactions were used to study polymer miscibility. Four para-substituted poly[(1-hydroxy-2,6-phenylene)methylenes] (*o,o*-PHMP's), viz., the H, Cl, NO_2, and *tert*-butyl derivatives, were synthesized and blended with poly(methyl methacrylate) (PMMA). Hydrogen bond dissociation energies were determined by Fourier transform infrared spectroscopy (FT-IR) and interaction characteristics were determined by differential scanning calorimetry, (DSC). The hydrogen-bonding interaction between the various PHMP's and PMMA was manifested by a shift of ~ 25 cm^{-1} in the infrared stretching frequency of the carbonyl group. The acidic strength and size of the substituent on the PHMP have a direct effect on the hydrogen-bonding strength in the blend. Blends of all systems show single T_g's and their magnitudes indicate slightly stronger hydrogen-bonding interaction effects for the *p*-NO_2- and *p*-Cl-PHMP's.

Introduction

There is increasing interest in understanding specific interactions in polymer blends because they play an important role in achieving compatibility.[1-3] Hydrogen bonds based on proton donor-acceptor interactions have been credited to yield miscibility in many systems.[4] Compatibility may be investigated by Fourier transform infrared (FT-IR) spectroscopy[5] and differential scanning calorimetry (DSC)[6] as well as other techniques.

Various novolac resins have been previously found to be compatible with polymers containing ether, nitrile, sulfone, and carbonyl groups.[6] In this paper, four poly[(1-hydroxy-2,6-phenylene)methylenes] (*o,o*-PHMP's) were

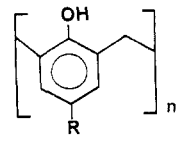

R = H, *t*-Bu, NO_2, Cl

o,o-PHMP

synthesized and characterized for blending studies with poly(methyl methacrylate) (PMMA). These studies were conducted to gain insight into the effect of the strength

0024-9297/86/2219-0973$01.50/0

of hydrogen bonding on miscibility. It has been demonstrated by pK_a determination that the acid strength of various substituted phenols and PHMP's is characteristic of the type of substituent present.[7] Direct evidence of hydrogen-bonding interactions of the PMMA carbonyl and the PHMP hydroxyl group for all PHMP blends was seen in the infrared. The presence of a second carbonyl absorption peak occurring approximately 25 cm^{-1} from the free carbonyl absorption peak was noted. The magnitude of the hydrogen-bonded shift is insensitive to the type of substituent. But, the relative intensity and area of the hydrogen-bonded carbonyl are quite different between PHMP blends. This suggests that the relative strength or the amount of hydrogen-bonded interaction in each of the PHMP blends might be different.

Experimental Section

The PMMA (Aldrich) used in this study has an intrinsic viscosity of 0.361 dL/g in benzene at 30 °C and a glass transition temperature (T_g) of 104.8 °C. Synthesis of poly[(1-hydroxy-2,6-phenylene)methylenes] (*o,o*-PHMP's) were performed by conventional condensation reactions between the respective substituted phenol and formaldehyde,[7] and the *o,o*-PHMP's were characterized by FT-IR, FT-NMR, and vapor phase osmometry.

Infrared Measurements. Thin films of 90/10 wt % PHMP/PMMA blends for FT-IR studies were cast from 2% 95/5 methylene chloride/tetrahydrofuran solutions (by weight) onto reflective aluminum plates by spin-casting techniques at room temperature. The films were transferred to a vacuum oven at 50 °C for 72 h to completely remove residual solvent. Infrared spectra were obtained on a Digilab FTS-20/B FT-IR spectrometer equipped with a liquid-nitrogen-cooled MCT detector. The aluminum reflectance plates were mounted on a Wilks specular reflectance apparatus with a cartridge heater attached, and spectra were obtained in an external reflection–absorption mode. Data were taken at a number of temperatures between 20 and 200 °C. Prior to data collection, the films were equilibrated for 5 min at each temperature. Temperature was controlled by using an Omega 4001KC temperature controller, within an accuracy of ±1 °C, with a chromel–alumel thermocouple held at the surface of the film by a mask with a 11-mm-i.d. window. Two hundred scans at a resolution of 2 cm^{-1} were signal averaged at the desired temperature and stored on a magnetic disk system. The frequency scale is internally calibrated with a reference helium–neon laser to an accuracy of 0.2 cm^{-1}. All films used in this study were sufficiently thin (10 μm) to be within an absorbance range where the Beer–Lambert law is obeyed.

Model studies were conducted in freshly distilled spectroscopic grade carbon tetrachloride (Aldrich) at blend concentrations of 0.05 M phenolic and 0.03 M methyl isobutyrate, where self-association does not exist. Phenolic compounds 2,6-dimethylphenol (Aldrich) and *p*-chlorophenol (Aldrich) were sublimed prior to use. A Barnes liquid cell was used with KBr windows and a path length of 0.5 mm. Temperature studies were performed with the aid of the temperature controller and thermocouple mentioned above to heat the liquid cell, which was wrapped with a heating tape. Heating did not exceed 50 °C, and data were taken as described above.

Differential Scanning Calorimetry (DSC) Measurements. Blends were prepared over the entire composition range from a 2% 95/5 methylene chloride/tetrahydrofuran solution (by weight) and cast onto Teflon sheets. Films were kept at ambient conditions for 6 h and then placed into a vacuum oven at 50 °C for 72 h to completely remove residual solvent. Glass transition temperatures were measured on a Du Pont 1090 differential scanning calorimeter. The glass transition temperature was taken as the extrapolated onset of the abrupt increase in the specific heat. This method was chosen due to the broad transition that occurred with the blends and it proved to be the most reliable. Samples were first heated at 150 °C in a silicone oil bath for 10 min and then quenched by powdered dry ice to introduce the same thermal history in each sample. Samples were then placed into the DSC in a nitrogen atmosphere and heated at 10 °C/min to 200 °C, and their thermograms were recorded. Glass transition temperatures were reproducible to within ±1 °C.

Results and Discussion

To explore the relative strength of the hydrogen-bonded interaction, efforts were directed toward elucidating the behavior of the free carbonyl–hydrogen-bonded carbonyl equilibrium by FT-IR techniques. Temperature studies were conducted on thin films by specular reflectance. Due to the complicated nature of the hydroxyl group interactions, where both self-association and association with PMMA occur, the carbonyl region was chosen to monitor the change in hydrogen-bonding interactions. For determining the thermodynamic parameters of hydrogen bond dissociation, the ratio of the relative peak intensity of free carbonyl to hydrogen-bonded carbonyl was followed with temperature utilizing Beer's law. From thermodynamic considerations, the equilibrium expression can be represented as

$$[\text{OH}\cdots\text{O}{=}\text{C}] \rightleftharpoons [\text{OH}] + [\text{C}{=}\text{O}] \quad (1)$$

with a dissociation constant K_d

$$K_d = [\text{OH}][\text{C}{=}\text{O}]/[\text{OH}\cdots\text{O}{=}\text{C}] \quad (2)$$

The dissociation constant can be expressed as

$$K_d = \exp(-\Delta H/RT + \Delta S/R) \quad (3)$$

where the variables have their usual meanings. Therefore

$$\ln K_d = -\Delta H/RT + \Delta S/R \quad (4)$$

and a van't Hoff plot of the logarithm of the dissociation constant vs. reciprocal temperature allow the determination of ΔH and ΔS.

The method chosen to calculate K_d is that of Ogura and Sobue,[8] which assumes that the ration of the extinction coefficients ($\epsilon_{\text{free}}:\epsilon_{\text{H bonded}}$) does not vary significantly with temperature. Therefore, the ratio of the two peak absorbances should give the relative fraction of free carbonyl groups which can be related to the hydrogen bond dissociation energy.

It has been pointed out that the absorption coefficients are very strongly dependent on frequency, so that if the frequency changes with temperature then they are indeed a factor to consider in the thermodynamic calculations.[9] To check this point the total integrated absorbance was determined for the carbonyl region to see if the extinction coefficients were actually changing or if the band shape was being influenced by temperature. In Figure 1 it is shown that there is only a small change, (about 2.5%), in the total area of the carbonyl bands in the temperature range of interest. In contrast, the hydrogenbonded carbonyl area decreases dramatically while the free-carbonyl area increases with increasing temperature. The shape of the entire carbonyl band narrows with increasing temperature as hydrogen bonding decreases. This is illustrated in Figure 2 by the plot of carbonyl half-width vs. temperature. Peak position for the free-carbonyl band remains constant, while the hydrogen-bonded carbonyl shifts about 5 cm^{-1} to higher frequency, over the entire temperature range.

Figure 3 illustrates the peak absorbances of the free and hydrogen-bonded bands as a function of temperature. The shape of this curve shows symmetrical characteristics of increasing free carbonyl with compensating decrease in hydrogen-bonded carbonyl from 120 to 200 °C. In Figure 4, a plot of the hydrogen-bonded intensity vs. the free intensity of the carbonyl band is shown with a slope of −1.05 in the temperature range 140–180 °C; this describes the behavior of the extinction coefficients with temperature. The observed linearity suggests that the extinction

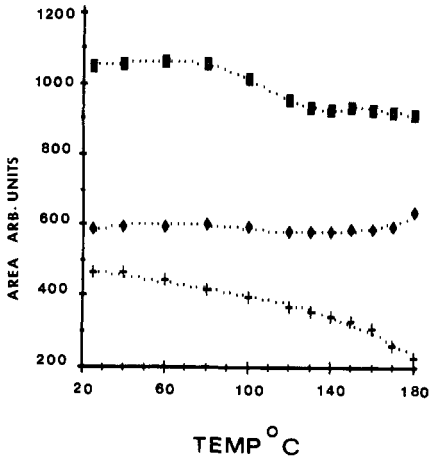

Figure 1. Plot of area vs. temperature for the (a) H-bonded (+), (b) free (♦) and (c) total C=O band (■) of p-NO_2-PHMP/PMMA blend.

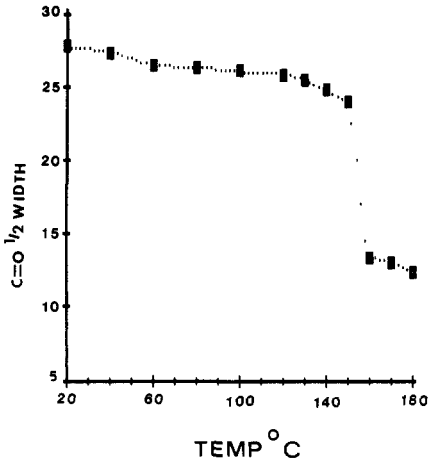

Figure 2. Plot of carbonyl half-width vs. temperature of p-NO_2-PHMP/PMMA blend.

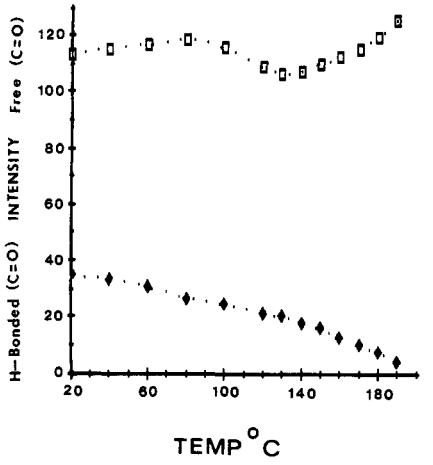

Figure 3. Plot of intensity of free (□) and H-bonded (♦) C=O bands vs. temperature of p-NO_2-PHMP/PMMA blend.

coefficients either are independent of temperature or have the same temperature dependence. The ratio of free carbonyl to hydrogen-bonded carbonyl peak intensities shows a change in temperature dependence as the glass transition temperature is approached. An abrupt change takes place at approximately 137 °C for the p-NO_2-PHMP/PMMA blend as seen in Figure 5. This inflection point or "break point" agrees well with the T_g determined by DSC (134.8 °C). Ogura and Sobue have proposed that the "break point", which corresponds to the T_g of the

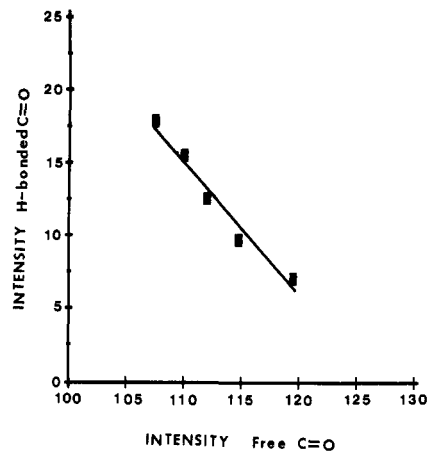

Figure 4. Plot of H-bonded intensity vs. free intensity of C=O band for p-NO_2-PHMP/PMMA blend.

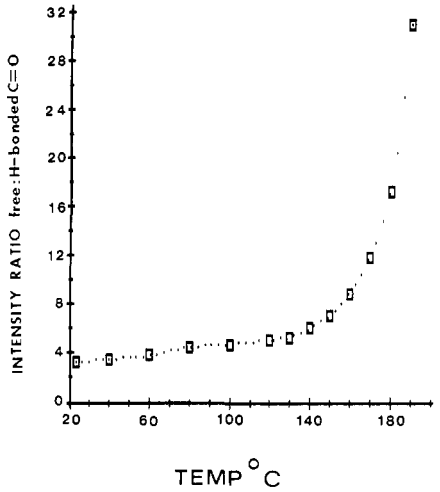

Figure 5. Plot of free/H-bonded C=O band intensity Ratio vs. temperature of p-NO_2-PHMP/PMMA blend.

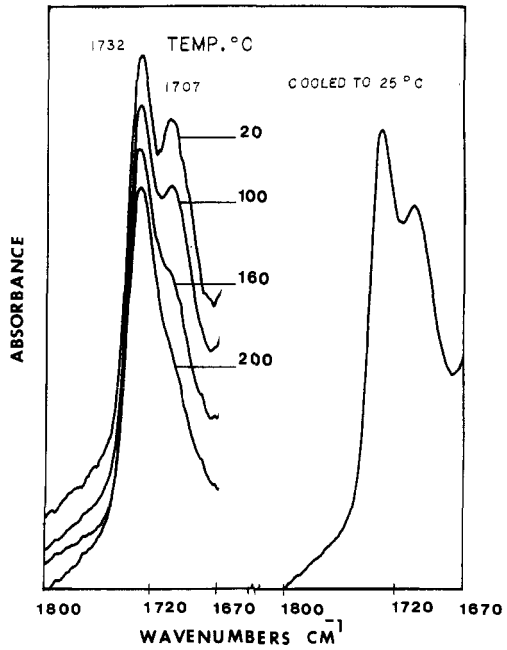

Figure 6. FT-IR spectra from 1670 to 1800 cm^{-1} recorded as a function of temperature of p-H-PHMP/PMMA blend.

blend, is associated with the initial breakdown of intermolecular hydrogen bonding.[8]

Each of the systems shows reversibility upon slow cooling as seen in Figure 6. This illustrates the reasso-

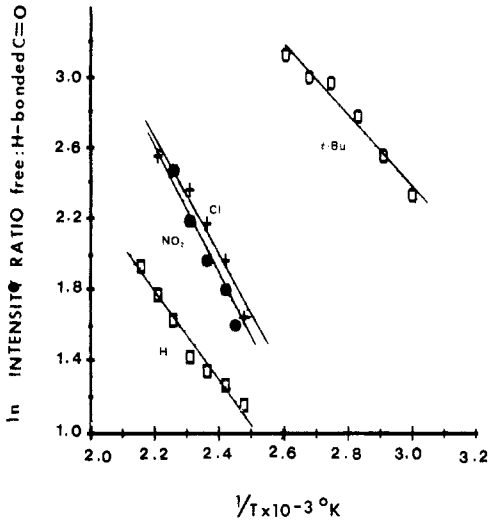

Figure 7. van't Hoff plots of ln [free/H-bonded C=O intensity ratio] vs. reciprocal temperature for (a) *p*-H- (□), (b) *p*-Cl- (+), (c) *p*-NO_2- (●), and (d) *p*-*t*-Bu-PHMP's/PMMA (○) blends.

Table I
Thermodynamic Parameters for Hydrogen Bond Dissociation in PMMA/PHMP Blends

o,o-PHMP	$-\Delta H$,[a] kcal/mol	ΔS, eu
p-H	5.06 ± 0.33	16.42 ± 0.38
p-Cl	5.64 ± 0.57	20.35 ± 0.65
p-NO_2	7.10 ± 0.85	22.51 ± 1.01
p-*t*-Bu	4.06 ± 0.36	18.60 ± 0.50

[a] Enthalpy from intensity calculation (eq 4).

ciation of the hydrogen-bonded carbonyl in the limit of the T_g. Hydrogen bond dissociation energies were calculated for temperatures above T_g by linear regression analysis on van't Hoff plots (Figure 7) with correlation coefficients greater than 0.980. Hydrogen bond dissociation energies (Table I) range from 4 to 7 kcal/mol for *p*-*t*-Bu- to *p*-NO_2-*o,o*-PHMP's, respectively. These values are reasonable and are in good agreement with the studies of MacKnight[10] and Ogrua.[8] They have determined the hydrogen-bonding strength by infrared spectroscopy in ethylene-methacrylic acid and styrene–methacrylic acid copolymers as 6 and 7 kcal/mol, respectively.

The data indicate that the strength of the hydrogen-bonding interaction is dependent upon the type of substituent. The order NO_2 > Cl > H > *tert*-butyl can be correlated with acidic strength and the electron-withdrawing effect of the substituent (Figure 8). In the case of the *p*-*t*-Bu-*o,o*-PHMP/PMMA blend, there seems to be a steric constraint affecting the blend. This is evident from the absorption of the hydrogen-bonded carbonyl. The relative area and magnitude of the peak intensity are considerably less than those of the other PHMP's. This suggests that interaction is affected by the presence of the bulky *tert*-butyl group at the para position. Therefore, as we had originally expected based on previous acid-base calculations, the type of substituent present on the PHMP does affect the hydrogen-bonding strength with PMMA.

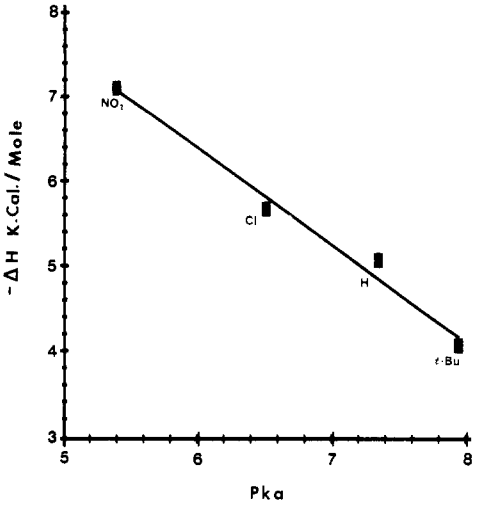

Figure 8. H-bond dissociation energy (kcal/mol) vs. pK_a.

Studies of the model compounds 2,6-dimethylphenol (2,6-DMP) and *p*-chlorophenol (p-Cl) with methyl isobutyrate (MIB) in a CCl_4 solution showed a 176- and 202-cm^{-1} shift in the hydroxyl group, respectively. A 26-cm^{-1} shift to lower wavenumber occurred in the carbonyl band for both of the model compounds with MIB. van't Hoff calculations using the carbonyl band with temperature gave hydrogen bond dissociation energies similar to that of the *p*-H-PHMP/PMMA blend as seen in Tables I and II. An empirical approximation developed by Drago[11,12] correlates the magnitude of the hydroxyl group shift to hydrogen bond dissociation energy

$$-\Delta H = 0.0103\Delta\nu_{OH} + 3.08 \quad (5)$$

where $\Delta\nu_{OH}$ is the shift in wavenumbers of the hydroxyl group due to hydrogen bonding and ΔH is the enthalpy of hydrogen bond dissociation. Reasonable enthalpies of dissociation were obtained from both functionalities and were compared with the respective PHMP/PMMA blends (Table II).

The glass transition temperatures for the blends show three types of results where the T_g's are higher (case 1), lower (case 2), and higher/lower (case 3) than the calculated weight-average values of T_g. The largest magnitude of deviation from the weight-average value is approximately 12 °C. In both cases 1 and 2, deviations from weight-average values may be represented by the product of the weight fractions of the individual components[13]

$$T_{gb} = W_1T_{g1} + W_2T_{g2} + qW_1W_2 \quad (6)$$

The term qW_1W_2 can be interpreted as the contribution of hydrogen bonds, which may be viewed as a pseudo-cross-link, and the increase in T_g due to such interactions can be related to the number of cross-links when the cross-link density is small. The term q is an indication of the efficacy of hydrogen bond formation. The q values obtained for the *p*-NO_2 and *p*-Cl blends are similar and slightly higher than those of *p*-H and *p*-*t*-Bu blends (Table III). The T_g results for the *p*-*t*-Bu and *p*-NO_2 blends show

Table II
Infrared Studies of Substituted Phenols with Methyl Isobutyrate

	ν_{OH}[a]			$\nu_{C=O}$		$-\Delta H$,[b]	$-\Delta H$,[c]
compd	free	bonded	diff	free	bonded	kcal/mol	kcal/mol
2,6-DMP[d]	3621.34	3444.86	176.48	1740.75	1714.71	4.97 ± 0.53	4.90 ± 0.53
p-Cl[e]	3609.77	3407.52	202.52	1740.75	1714.71	5.34 ± 0.72	5.17 ± 0.72

[a] Frequency (cm^{-1}). [b] Enthalpy from area calculations (eq 4). [c] Enthalpy from Drago approximation (eq 5). [d] 2,6-Dimethylphenol. [e] *p*-Chlorophenol.

Table III
Differential Scanning Calorimetry and Number-Average Molecular Weight Data

PHMP	T_g, °C	M_n	M_{n_0}	X_n	q	k
p-H	89.9	1080	106	10.2	40.12	0.892
p-Cl	87.5	744	140	5.3	44.82	1
p-NO_2	134.8	833	151	5.5	−41.94	1
p-t-Bu	108.8	917	162	5.7	−39.42	1.02

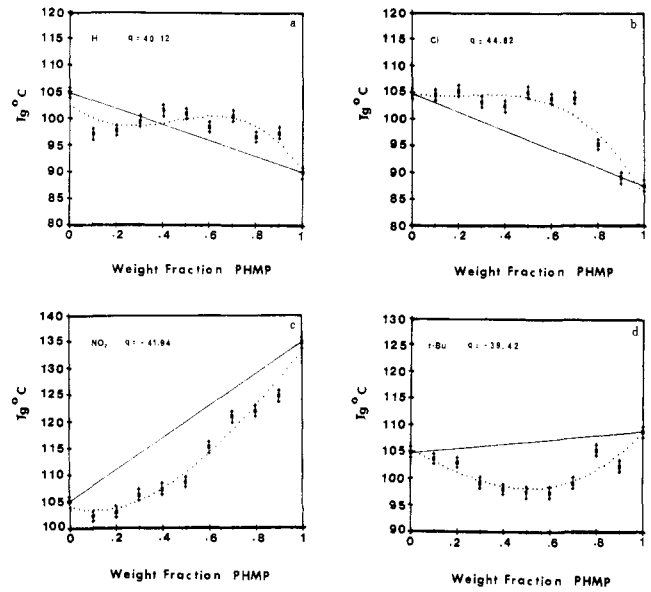

Figure 9. DSC plots of glass transition temperature (T_g) vs. weight percent PHMP: (a) p-H; (b) p-Cl; (c) p-NO_2; (d) p-t-Bu. (—) weight-average values; (···) eq 7; (■) DSC data.

case 2 type behavior, while p-Cl shows case 1 type behavior. The results for the p-H blend are different from those of the other PHMP blends and show case 3 type behavior. The T_g of the blends falls below the weight-average values at low concentrations of PHMP but exceeds the weight-average values at higher concentrations (Figure 9). This S-shaped curve can be fitted by

$$T_{gb} = \frac{W_1 T_{g1} + kW_2 T_{g2}}{W_1 + kW_2} + qW_1 W_2 \qquad (7)$$

which is a more general version of eq 6.

The structures of both o,o-PHMP's and PMMA are fairly rigid. However, cyclic ring structures are known to exist for such oligomeric PHMP's.[14] When small amounts of the o,o-PHMP component are present, they act as a diluent in which there is a high local concentration of hydrogen-bonded segments separated by large regions of pure PMMA. The distribution of hydrogen bonds in the mixture is inhomogeneous. Some of the PMMA molecules may have only a few hydrogen bonds attached to parts of the molecule, due to steric and spatial constraints. The restrictions imposed by such nonuniformly distributed hydrogen bonds give rise to glass transitions that show slight deviations from the weight-average values. When large amounts of PHMP are present in the blend, they give rise to more ramdomly distributed hydrogen bonds and as a result produce greater deviations in the glass transition temperatures as compared to the weight-average values.

Conclusions

From the infrared results the nature and size of the substituent on the PHMP do affect the hydrogen bond dissociation energy in the order of NO_2 > Cl > H > t-Bu. The acidic strength of the various PHMP's correlates inherently with the hydrogen-bonding strength. DSC results reveal that the relative number of interaction sites (q) for p-NO_2- and p-Cl-o,o-PHMP's is slightly greater than that for p-H- and p-t-Bu-o,o-PHMP's. However, the q value obtained is the net sum of all types of interactions, self-association between PHMP, and intermolecular association between PHMP and PMMA. The similar q values obtained indicate the incorporation of the PHMP/PHMP self-association and separation of this effect is not possible. The region of the glass transition temperature can be associated with the onset of the breakdown of intermolecular hydrogen bonding between chains as illustrated by the "break point" in Figure 5. This has also been proposed by Ogura and Sobue.[8] These hydrogen-bonding systems show reassociation upon slow cooling above the T_g of the blend. Differences in enthalpy of dissociation values are relatively small between PHMP blends, yet they are noticeable and show behaviorable trends that correlate with their pK_a data. Understanding the nature and effect of substitution on hydrogen bonding in blends may be very useful for tailoring future systems to gain enhanced properties.

Acknowledgment. This work was supported in part by a grant from the National Science Foundation (Grant DMR-8303499), the Polymer Research Institute of New York (Polymers Program), and the Industrial Technology Research Institute of Taiwan. We thank Frank DeBlase for helpful suggestions.

Registry No. PMMA (homopolymer), 9011-14-7; (formaldehyde)·(phenol) (copolymer), 9003-35-4; (formaldehyde)·(*p*-*tert*-butylphenol) (copolymer), 25085-50-1; (formaldehyde)·(*p*-nitrophenol) (copolymer), 27322-28-7; (formaldehyde)·(*p*-chlorophenol) (copolymer), 26045-03-4.

References and Notes

(1) Olabisi, O.; Robeson, L. M.; Shaw, M. T. "Polymer–Polymer Miscibility"; Academic Press: New York, 1979.
(2) Krause, S. "Polymer Blends"; Paul, D., Newman, S., Eds.; Academic Press: New York, 1978.
(3) Fowkes, F. M.; Tischler, D. O.; Wolfe, J. A.; Lannigan, L. A.; Ademu-John, C. M.; Halliwell, M. J. *J. Polym. Sci., Polym. Chem. Ed.* **1984**, *22*, 547.
(4) Cangelosi, F.; Shaw, M. T. *Polym. Plast. Technol. Eng.* **1983**, *21*, 13.
(5) Coleman, M. M.; Zarian, J. *J. Polym. Sci., Polym. Phys. Ed.* **1979**, *17*, 837.
(6) Fahrenholtz, S. R.; Kwei, T. K. *Macromolecules* **1981**, *14*, 1076.
(7) DeRosa, T.; Pearce, E. M.; Charton, M. *Macromolecules* **1985**, *18*, 2277.
(8) Ogura, K.; Sobue, H. *Polym. J.* **1972**, *3*, 153.
(9) Coleman, M. M.; Skrovanek, D. J.; Howe, S. E.; Painter, P. *Macromolecules* **1985**, *18*, 301.
(10) Earnest, T. R., Jr.; MacKnight, W. J. *Macromolecules* **1980**, *13*, 844.
(11) Drago, R. S.; O'Bryan, N.; Vogel, G. C. *J. Am. Chem. Soc.* **1970**, *92*, 3924.
(12) Drago, R. S.; Epley, T. D. *J. Am. Chem. Soc.* **1969**, *91*, 2883.
(13) Kwei, T. K. *J. Polym. Sci., Polym. Lett. Ed.* **1984**, *22*, 307.
(14) Tobiason, F. *J. Polym. Sci., Polym. Chem. Ed.* **1979**, *17*, 949.